



## Inflammation-Stimulated Mesenchymal Stromal Cell-Derived Extracellular Vesicles Attenuate Inflammation

MATTHEW T. HARTING <sup>a</sup>, AMIT K. SRIVASTAVA,<sup>a</sup> SIQIN ZHAORIGETU,<sup>a</sup> HENRY BAIR,<sup>a</sup> KARTHIK S. PRABHAKARA,<sup>a</sup> NAAMA E. TOLEDANO FURMAN,<sup>a</sup> JODY V. VYKOUKAL,<sup>b</sup> KATHERINE A. RUPPERT,<sup>a</sup> CHARLES S. COX JR.,<sup>a</sup> SCOTT D. OLSON <sup>a</sup>

**Key Words.** Mesenchymal stromal cells • Mesenchymal stem cells • Extracellular vesicles • Exosomes • Microvesicles • Inflammation • Current good manufacturing practices

<sup>a</sup>Department of Pediatric Surgery, University of Texas McGovern Medical School, Houston, Texas, USA;

<sup>b</sup>McCombs Institute for the Early Detection and Treatment of Cancer, The University of Texas MD Anderson Cancer Center, Houston, Texas, USA

Correspondence: Matthew T. Harting, M.D., M.S., Department of Pediatric Surgery, University of Texas McGovern Medical School, Houston, 6431 Fannin Street, MSB 5.233, Houston, Texas 77030, USA. Telephone: 713.500.7300; e-mail: matthew.t.harting@uth.tmc.edu

Received January 23, 2017; accepted for publication October 22, 2017; first published online in *STEM CELLS EXPRESS* October 27, 2017.

<http://dx.doi.org/10.1002/stem.2730>

### ABSTRACT

Extracellular vesicles (EVs) secreted by mesenchymal stromal cells (MSCs) have been proposed to be a key mechanistic link in the therapeutic efficacy of cells in response to cellular injuries through paracrine effects. We hypothesize that inflammatory stimulation of MSCs results in the release of EVs that have greater anti-inflammatory effects. The present study evaluates the immunomodulatory abilities of EVs derived from inflammation-stimulated and naive MSCs (MSCEv<sup>+</sup> and MSCEv, respectively) isolated using a current Good Manufacturing Practice-compliant tangential flow filtration system. Detailed characterization of both EVs revealed differences in protein composition, cytokine profiles, and RNA content, despite similarities in size and expression of common surface markers. MSCEv<sup>+</sup> further attenuated release of pro-inflammatory cytokines in vitro when compared to MSCEv, with a distinctly different pattern of EV-uptake by activated primary leukocyte subpopulations. The efficacy of EVs was partially attributed to COX2/PGE<sub>2</sub> expression. The present study demonstrates that inflammatory stimulation of MSCs renders release of EVs that have enhanced anti-inflammatory properties partially due to COX2/PGE<sub>2</sub> pathway alteration. *STEM CELLS* 2018;36:79–90

### SIGNIFICANCE STATEMENT

Previous work has identified mesenchymal stromal cell-derived extracellular vesicles (MSCEv) as mediators of cell-cell communication and effectors of cellular/tissue change. This study isolated MSCEv using a clinically propitious filtration system after stimulation with inflammatory cytokines, characterized their composition, and evaluated their effect on inflammation, along with their potential mechanism of action and interaction with potential target cells. This study identified important compositional differences between control and stimulated MSCEv in cytokine and RNA content. Furthermore, stimulated MSCEv attenuate TNF- $\alpha$  and IFN- $\gamma$  release from activated splenocytes compared to standard MSCEv (and liposomal controls). The nature of MSCEv interaction with cells likely involves cellular internalization, so this study fluorescently labeled MSCEv prior to coculture with activated leukocytes to determine changes in uptake activity in response to several antigens. These studies demonstrate a specific anti-inflammatory, MSCEv-mediated response and the capacity to change efficacy in response to inflammatory cues, creating the foundation for enhancing the efficacy of translational efforts using MSCEv for targeting inflammatory injuries and diseases. This represents a new paradigm for generation of extracellular vesicles targeting specific pathologies.

### INTRODUCTION

Mesenchymal stromal cells (MSCs) are progenitor cells with burgeoning clinical and therapeutic potential that have previously been isolated from a number of tissues, usually by plastic adherence and expansion under specific culture conditions. As translational efficacy of MSCs has been realized in multiple disciplines,

numerous underlying general mechanisms of action have emerged, including inflammation modulation, angiogenesis, and cytoprotection [1–5]. These activities combine to form a central hypothesis that MSCs exert a dynamic homeostatic response that supports the preservation of tissue and recovery of function.

Extracellular vesicles (EVs) are small (40 nm–1  $\mu$ m) vesicles released by various cell

types, including MSCs, via endocytic or secretory pathways [6, 7]. EVs released by cells are a heterogeneous population characterized by their size, surrounding lipid bilayer, and associated markers, although specific physical and biochemical criteria remain nebulous [8, 9]. EVs derived from MSCs contain a number of growth factors, lipids, proteins and nucleic acids (mRNAs, pre-micro RNAs [miRNAs], miRNAs, and transfer RNA (tRNA)) [10, 11]. Transfer of these proteins, bioactive lipids, and nucleic acids to neighboring cells promotes cell-to-cell communication and can drastically modify the activity of target cells in physiological and pathological conditions to contribute to the paracrine (or endocrine) effect of MSCs [9, 12, 13]. For example, MSCs derived from bone marrow and umbilical cord blood have shown a strong capacity for EV secretion in response to cellular injuries [14, 15]. Similarly, MSC therapeutic efficacy has shown independence from engraftment, cellular differentiation, and physical proximity, leaving endocrine-like and paracrine factors as plausible mechanisms linking the cells and often distant target tissue effects [16]. The therapeutic efficacy of EVs has emerged as a strategy that may have advantages over a cellular therapeutic strategy. EVs are particularly interesting due to low malignant potential, cellular/tissue specificity, and potent immunomodulatory effects. Clinically, MSC-derived EVs are less likely to suffer the pulmonary first pass effect [17], which is important both for safety and for system-wide delivery to take place. The high potential for efficacy combined with a promising safety profile is rapidly driving EV translational efforts forward.

In this study, we used a highly scalable and current Good Manufacturing Practice (cGMP)-compliant tangential flow filtration (TFF) system to isolate EVs based on their size. We hypothesized that EVs derived from inflammation stimulated-MSCs (MSCEV<sup>+</sup>) would significantly attenuate proinflammatory cytokine production, compared with EVs derived from naïve MSCs (mesenchymal stromal cell-derived extracellular vesicles [MSCEV]). We observed that MSCs stimulated with proinflammatory cytokines to produce EVs with heightened immunomodulatory potential, an observation important to improve efficacy for future clinical application.

## MATERIALS AND METHODS

### Isolation and Culture of Human Mesenchymal Stromal Cells

Human mesenchymal stromal cells (hMSCs) were isolated from commercially available fresh human bone marrow aspirates of a 34-year-old female (AllCells, Alameda, CA) using density centrifugation and plastic adherence as previously described [18]. An adherent population of MSCs was obtained 3 weeks after the initiation of culture. The cells were screened for typical spindle-like morphology and growth kinetics. The cells were further expanded by plating  $10^6$  passage 2 cells at 200 cells/cm<sup>2</sup> in 2,528 cm<sup>2</sup> in Nunc Cell Factory Systems with complete culture medium (CCM) that consisted of  $\alpha$ -minimal essential medium (Life Technologies, Grand Island, NY), 17% fetal bovine serum (FBS; Atlanta Biologicals, Norcross, GA), 100 units/ml penicillin (Life Technologies, Carlsbad, CA), 100  $\mu$ g/ml streptomycin (Life Technologies, Carlsbad, CA), and 2 mM L-glutamine (Life Technologies). At 70% cell confluence, the medium was discarded, the cultures were washed with phosphate-buffered saline (PBS) (Life Technologies, Carlsbad, CA), and the adherent cells

harvested with 0.25% trypsin (Life Technologies, Carlsbad, CA) for 5 minutes at 37°C and frozen at  $10^6$  cells/ml for subsequent experiments as passage 3 cells [2] and characterized with data previously published [19].

### Stimulation of hMSCs

To stimulate the naïve hMSCs, cells were cultured in the CCM with TNF- $\alpha$  (20 ng/ml) + IFN- $\gamma$  (20 ng/ml) inflammatory cytokines cocktail overnight. After which, the medium was removed, cells were washed with PBS and fresh serum-free CCM was added. After culturing for another 48 hours, the medium was collected and used for EVs isolation.

### Isolation of EVs by Sequential Filtration

EVs were isolated from both naïve (MSCEV) and activated MSCs (MSCEV<sup>+</sup>). We used large format cell culture flasks, and cultured hMSCs (1,000 cells/cm<sup>2</sup>) to ~75% confluence over 5–6 days in 3,180 cm<sup>2</sup> Corning CellStack Systems (5 layer) to 500 ml serum-free CCM at a time by approximately  $18\text{--}25 \times 10^6$  hMSCs. After 48 hours of culture, the conditioned media was collected and pre-filtered through a 0.2  $\mu$ m membrane to remove floating cells and cell debris. The filtered media was then loaded into the Millipore LabScale TFF system equipped with a Biomax 500 kDa (5  $\mu$ m) Pellicon filter (Millipore, Billerica, MA). We conducted three volume exchanges with PBS with a target feed pressure below 20 psi and retentate pressure below 10 psi. A final volume reduction step was then performed, with EVs recovered in a final volume of approximately 7–10 ml of PBS. Between uses, the equipment and filter were flushed with PBS, cleaned using 0.1 N NaOH, and refilled with PBS. This allowed large volumes of conditioned media to be concentrated into an EV-enriched solution appropriate for use both in vitro and in vivo (Fig. 1).

### Transmission Electron Microscopy

Morphologies of EVs and empty liposomes were visualized using transmission electron microscopy (TEM). EVs and empty liposome suspensions (5  $\mu$ l each) were applied to a 300 mesh copper Formvar-carbon coated electron microscopy grids and left at room temperature for 15 seconds. The excess suspension was blotted gently on Whatman no.1 filter paper. The grids were the negatively stained using 5  $\mu$ l of 1.5% uranyl acetate, air-dried, and screened using a JEOL 1200EX transmission electron microscope at 60 kV. Multiple 2k  $\times$  2k images were recorded using a Gatan 830 Orius CCD camera.

### Particle Size Distribution and Quantification

Samples of EVs were quantified via Brownian diffusion size analyses using ZetaView instrumentation (Particle Metrix, Germany). Sample aliquots were diluted  $10^2\text{--}10^6$ -fold to achieve optimal concentration for analysis; 1.0 ml of diluted sample was used for each analysis. Light scattering of individual particles in solution was digitally recorded, particle trajectory and displacement was automatically analyzed by image analysis tracking software, and the particle-size distribution was determined from the observed Brownian motion of individual particles according to the Stokes-Einstein relationship.

### Western Blot Assay

The EV proteins were denatured in Laemmli sample buffer at 100°C for 5 minutes. Proteins were separated by using 4%–

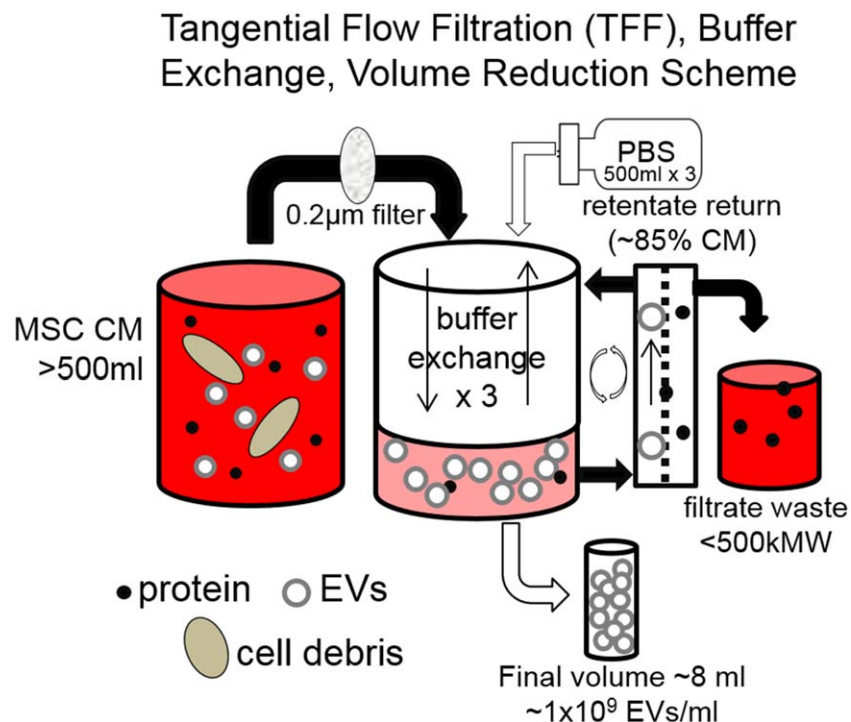


**Figure 1.** EV isolation technique—Tangential flow filtration and volume reduction. Conditioned, serum-free media (CM) from cultures of MSCs are passed through a 0.2 µm filter to remove cells, cellular fragments, and large protein aggregates. Tangential flow filtration with a 500 kMW Pellicon filter progressively removes free protein and reduces the volume to an ~30% of the initial volume. When the volume reaches an ~50 ml, PBS is used to replace the lost volume a total of three times as a buffer exchange. A final volume reduction will concentrate the resulting EV-enriched solution to approximately 8–12 ml at a concentration of an  $\sim 1 \times 10^9$  EV/ml. Abbreviations: CM, conditioned media; EV, extracellular vesicle; MSC, mesenchymal stromal cell; PBS, phosphate-buffered saline.

15% sodium dodecyl sulfate polyacrylamide gel electrophoresis and transferred to Immun-Blot membrane (Bio-Rad, Hercules, CA), which were then incubated with primary antibodies CD63 (Santa Cruz), CD9 (Santa Cruz, Dallas, TX), CD81 (Santa Cruz, Dallas, TX) HSP70 (Santa Cruz, Dallas, TX), LAMP-1 (CD107a) (Santa Cruz, Dallas, TX), and COX2 (Abcam, Cambridge, UK), respectively. Subsequently, the blots were incubated with respective horseradish peroxidase-labeled secondary antibodies (Bio-Rad, Hercules, CA). Proteins were detected using enhanced chemiluminescence (Amersham) and Western blotting detection system (Amersham Biosciences, Piscataway, NJ).

#### Flow Cytometry of EVs

Protein content of both MSCEv and MSCEv<sup>+</sup> were determined using standard Bradford assay (BioRad, Hercules, CA). EVs were retrieved and purified using Exosome-human CD63 isolation/detection kit (Invitrogen, Carlsbad, CA). Briefly, 100 µl of EV solution was added with 200,000 washed magnetic beads and incubated overnight at 4°C with mixing. The next day, the beads were collected and washed twice using the DynaMag.

Antibodies were added to the purified EVs and incubated in the dark for 45 minutes at room temperature on a sample shaker. The antibodies used were: APC antihuman CD63, Alexa Fluor 488 antihuman CD107a (LAMP-1), and PE antihuman CD9, all purchased from Biolegend (San Diego, CA). Beads-bound EVs were washed and run on BD LSRII Flow Cytometer (BD Biosciences). The assay was performed in triplicate. Analysis of the bead-bound EVs was performed using Kaluza

analysis software (Beckman Coulter, Brea, CA) versus unstained and isoclonic controls for each marker.

Additional flow cytometry was performed for typical MSC phenotype, including CD73-PE, CD90-BV421, CD105-FITC, CD31-APC, CD44-FITC (BD Biosciences), CD34-APC, CD45-APC-Cy7, CD29-PE (Biolegends) in two sets of panels on the BD LSRII Flow Cytometer (BD Biosciences).

#### RNA Protection Assay

The ability of the lipid bilayer to protect RNA from degradation was measured using a technique modified from a number of previous publications [20, 21]. Briefly, 100 µl samples of EV were incubated with an additional 400 µl of a digestion mixture for a final volume of 100 µl containing 100 U/ml RNase A ±1% Triton X-100 for 30 minutes at room temperature. RNA was then isolated using a commercial ZR RNA Mini-prep kit (Zymo Research, Irvine, CA) and RNA concentration was analyzed using a Qubit fluorometer and the Qubit RNA BR assay kit (Fisher Scientific).

#### Next Generation Sequencing

Total RNA was isolated from EVs using miRCURY RNA Isolation Kit (Exiqon, MA) following the manufacturer's protocol. Purified RNA at a concentration of 200 ng/µl was suspended in RNase free water for further analysis.

Next generation sequencing libraries were generated with the TailorMix Micro RNA Sample Preparation version 2 protocol (SeqMatic LLC, CA). A cDNA library was amplified via enrichment polymerase chain reaction (PCR) and final RNA library was

size-selected. RNA sequencing was performed on the Illumina HiSeq 2500 Ultra-High-Throughput Sequencing System.

Data analysis was performed using a basic local alignment search tool (BLAST) search was performed at the National Center for Biotechnology Information (NCBI) database using BLAST 2.2.30, and number of reads that aligned to any of the RNA was calculated. Hits with 100% identity and matching the whole length of RNA was used in this study. Bioconductor's DESeq package will be then used for differential expression analysis.

### Cytokine Array

A commercial cytokine array was purchased from R&D Systems (Minneapolis, MN) and used according to the manufacturer supplied protocol and as previously described [22, 23]. Briefly, whole EV protein was isolated using RIPA buffer (Thermo Scientific) and analyzed using the Proteome Profiler Human Cytokine Array Kit (ARY005B, R&D Systems, Minneapolis, MN) which simultaneously measures the presence and relative abundance of 36 cytokines and chemokines. This elidot-style array was quantified using chemiluminescence and analyzed using ImageJ (NIH).

### Primary Splenocyte Inhibition/Activation Assay

Rats were purchased from Harlan (Indianapolis, IN) for use in this study. The animals were housed on a 12 hours light/dark cycle with ad libitum access to food and water. All protocols involving the use of animals were in compliance with the National Institutes of Health Guide for the Care and Use of Laboratory Animals and were approved by the Institutional Animal Care and Use Committee (HSC-AWC-13-065 and HSC-AWC-12-059). Splenocyte preparation was performed as previously described [23]. Briefly, after obtaining a fresh spleen from male Sprague Dawley rats (250–300 g) under anesthesia, the spleen was morselized by pushing it through a 70  $\mu$ m mesh filter in order to exclude all connective tissue. The remaining material was suspended in ice cold PBS and centrifuged at 400 g for 8 minutes. Next, the supernatant was removed and the sample suspended in 5 ml of red blood cell lysis buffer (Sigma-Aldrich, St. Louis, MO) and allowed to incubate on ice for 5 minutes. Subsequently, the sample was diluted with 5 ml of PBS and centrifuged at 400 g for 8 minutes. The supernatant was again removed and the pellet suspended in phenol free RPMI with 10% FBS and titrated 8–10 times after which the sample was run through a 40  $\mu$ m mesh filter to remove any clumps. The splenocytes were counted and checked for viability via Trypan blue exclusion. Splenocytes ( $2 \times 10^5$  cells/ml) were activated with lipopolysaccharide (LPS) or concanavalin A (ConA), alone or in the presence of MSCs (1:20, MSC:splenocyte ratio) as previously described [23] in 96 well plates. Culture supernatant was collected 24 hours after LPS treatment or 72 hours after ConA activation and the samples analyzed using a TNF- $\alpha$  or IFN- $\gamma$  (Biolegend, CA) and PGE<sub>2</sub> (Cayman, MI) enzyme-linked immunosorbent assay (ELISA) kits following manufacturer's protocol. For COX-2 inhibition, a specific inhibitor NS-398 (70590, Cayman Chemicals) was used at 0.1 nM, 1 nM, and 10 nM concentrations, respectively.

### Peripheral Blood Mononuclear Cell-EV Interaction

MSCEv and MSCEv<sup>+</sup> were labeled with Exo-GLOW Exosomes labeling kits (System Biosciences, Palo Alto, CA), according to

the manufacturer's protocol, with some modifications. Briefly, we added 50  $\mu$ l 10 $\times$  Exo-Green to 500  $\mu$ l of resuspended EV pellets and incubated the solution in 37°C for 10 minutes. To stop labeling reaction, 100  $\mu$ l of the ExoQuick-TC reagent was added to the labeled EV sample suspension, mixed by inverting and placed on ice for 30 minutes. Finally, sample was centrifuged for 3 minutes at 14,000 rpm in a microfuge and supernatant was removed with excess label. The EV pellet was resuspend in 500  $\mu$ l PBS for further analysis.

For human peripheral blood mononuclear cells (PBMCs) isolation, blood was collected from a healthy donor (IRB approval number HSC-MS-10-0190) and diluted 1:1 with PBS and PBMC were collected using Ficoll-Paque gradient (GE Healthcare), according to manufacturer recommendation. PBMCs were activated for 24 hours with LPS (1 ng/ml, Invivo-gen), Concanavalin A (5  $\mu$ g/ml, Alfa Aesar), or CD3/CD28 T cell proliferation beads (Miltenyi Biotec), according to manufacturer recommendation. One million cells were incubated with Exo-Glow labeled MSCEv or MSCEv<sup>+</sup> for 2 hours at 37°C. Later, cells were washed and stained with CD45 APC-Cy7 (BD Pharmingen), CD3 APC (BD Pharmingen), CD4 PerCP-Cy5.5 (Millipore), and CD8 V450 (BD Horizon) for 20 minutes at room temperature. Samples were then analyzed on BD LSR II Flow Cytometer (BD Biosciences). Assuming cells' intensity of fluorescence signal correlates to the amount of EVs the cells uptake during that period of incubation. The results are presented as the averaged median value of the fluorescence intensity  $\pm$  SEM.

### Activin-A, Follistatin, and PAPP-A2 Assay

The levels of activin-A, follistatin, and PAPP-A2 in MSCEv and MSCEv<sup>+</sup> were determined using a commercially available ELISA kit (Ansh Labs LLC, Webster, TX) according to manufacturer's protocol.

### Statistical Analyses

For all the analyses, comparison among groups was made using one-way analysis of variance followed by post hoc comparison (Newman-Keuls multiple) test. Differences between the means were considered significant at  $p < .05$ . Results are shown as value  $\pm$  SD. Statistical analysis was done using the Graphpad Prism (7.0 software).

## RESULTS

### EV Characterization

Similar to other groups, we found that in order to harvest sufficient EVs to perform several assays, we had to use large-scale formats. Bone marrow-derived MSC at early passage (p3) were plated and grown to approximately 80% confluence in Corning 5-layer CellStack for a final density of approximately 10,000 cells/cm<sup>2</sup>. Cultures were then treated with TNF- $\alpha$  and IFN- $\gamma$  or serum-free media in parallel prior to conditioning serum-free media for 48 hours to harvest EVs using TFF. No gross changes in cell viability and division dynamics of MSCs under the stimulation of proinflammatory cytokines were observed. Isolation of the MSCEv and MSCEv<sup>+</sup> yielded approximately 80–160 EVs per cell per 48 hours. Following the TFF isolation and volume reduction, we reached a final

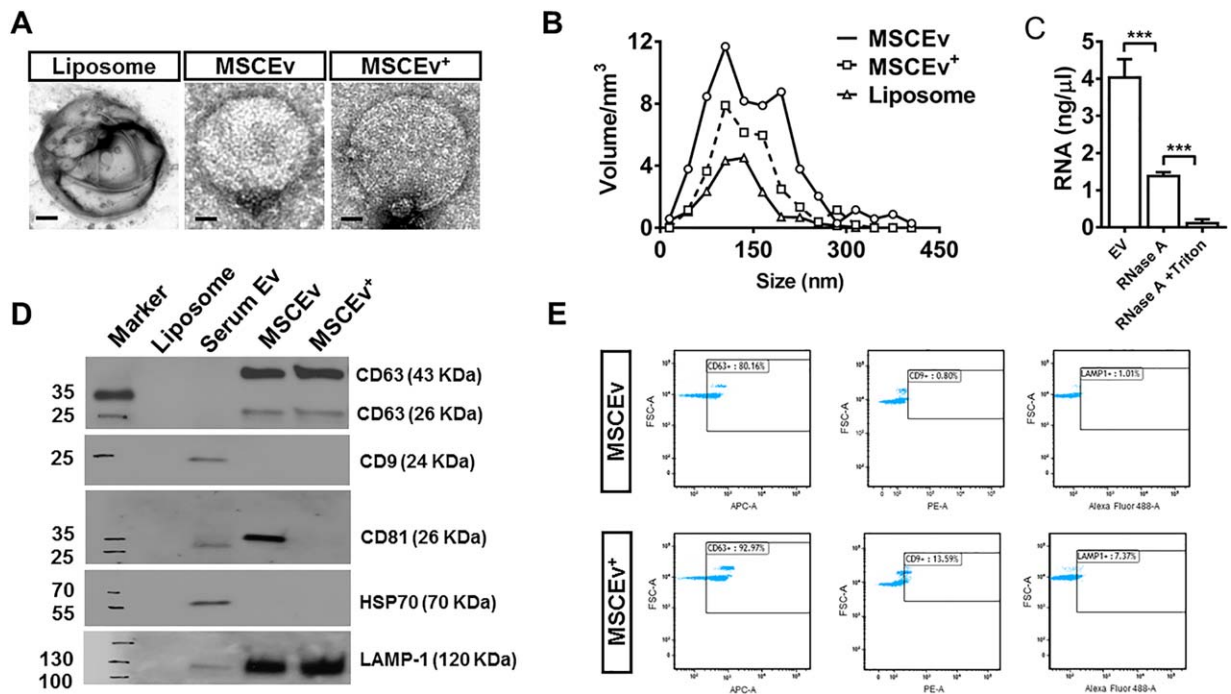


**Figure 2.** Mesenchymal stromal cell-derived EV characterization. (A): Qualitative characterization using transmission electron microscopy imaging (representative image shown, scale bar equals 20 nm), (B) RNA protection assay confirms lipid bilayer encapsulated RNA, (C) quantitative characterization of particle size and concentration using ZetaView (Particle Metrix), (D) Western blotting identification of EV-specific markers (CD63, CD9, CD81, HSP70, and LAMP-1), (E) flow cytometric identification of EV-specific markers (CD63, CD9, and LAMP-1). Abbreviation: EV, extracellular vesicle.

concentration of approximately  $1 \times 10^9$  EVs/ml (isolated from an ~30 million cells) in 8–10 ml of media.

Qualitative morphological characterization of EVs by TEM revealed mostly uniform sphere-shaped vesicles (Fig. 2A). There were no observed differences in the morphologies of MSCEv and MSCEv<sup>+</sup>. Liposomal controls (synthetic nanoparticles) were also structurally similar to both MSCEv and MSCEv<sup>+</sup> (Fig. 2A). We performed quantitative analysis of EVs using a nanoparticle tracking analyzer (ZetaView, Particle Metrix), which calculates a translational diffusion constant from the direct observation of Brownian motion to calculate particle size. Isolated EVs had a relatively homogenous size, as >90% of MSCEv and MSCEv<sup>+</sup> were in the 75–165 nm range, with the peak at ~100 nm (Fig. 2B). RNA was largely contained in EVs, as it was protected from degradation by RNase in the presence of an intact lipid bilayer (Fig. 2C). Western blot analysis comparing MSCEv and MSCEv<sup>+</sup> showed the consistent and equivalent presence of CD63 and CD107a (LAMP-1), while neither CD9 nor HSP70 were identified in either group. CD81 was identified in MSCEv, though not identified in MSCEv<sup>+</sup> (Fig. 2D). Using flow cytometry, we identified the presence of CD29, CD44, CD73, and CD105, classic MSC markers, as well as the absence of CD34, CD45, and HLA-DR on MSCEv (Supporting Information Table S1). The EV-specific marker CD63 was detected in both MSCEv and MSCEv<sup>+</sup>, though MSCEv<sup>+</sup> showed a 25% increased expression (Fig. 2E), while the expression of both CD9 and CD107a was detected at low levels.

The presence and relative amount of 34 inflammation-associated cytokines was analyzed using a commercial ELI-dot style array (Proteome Profiler, R&D Systems). The array

### Relative Protein Expression

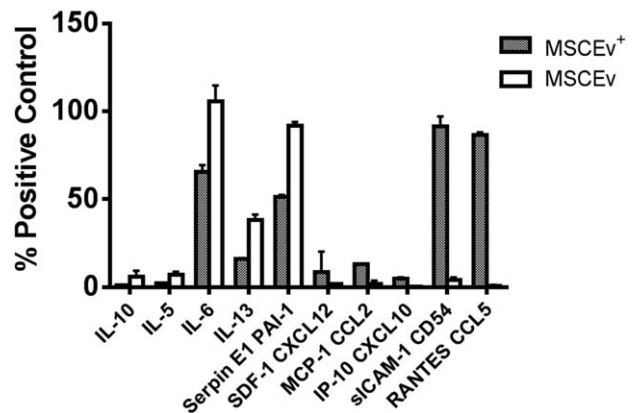


**Figure 3.** Inflammatory cytokine array for MSCEv. A membrane-based antibody array was used to assay relative quantities of 34 different cytokines associated with inflammation. Presented here are the cytokines with at least a threefold change up or down when normalized to the positive control.

identified a number changes in cytokine expression between MSCEv and MSCEv<sup>+</sup> (Fig. 3). Most notably, increases in the expression of ICAM 1, CXCL12, and CCL5 were identified in MSCEv<sup>+</sup>, whereas the expression of IL-5, IL-6, IL-10, and IL-13 were decreased.

### RNA Sequencing

High throughput RNA sequencing was performed to analyze global differences in RNA content of MSCEv<sup>+</sup> versus MSCEv. RNA sequences were sorted according to classification,

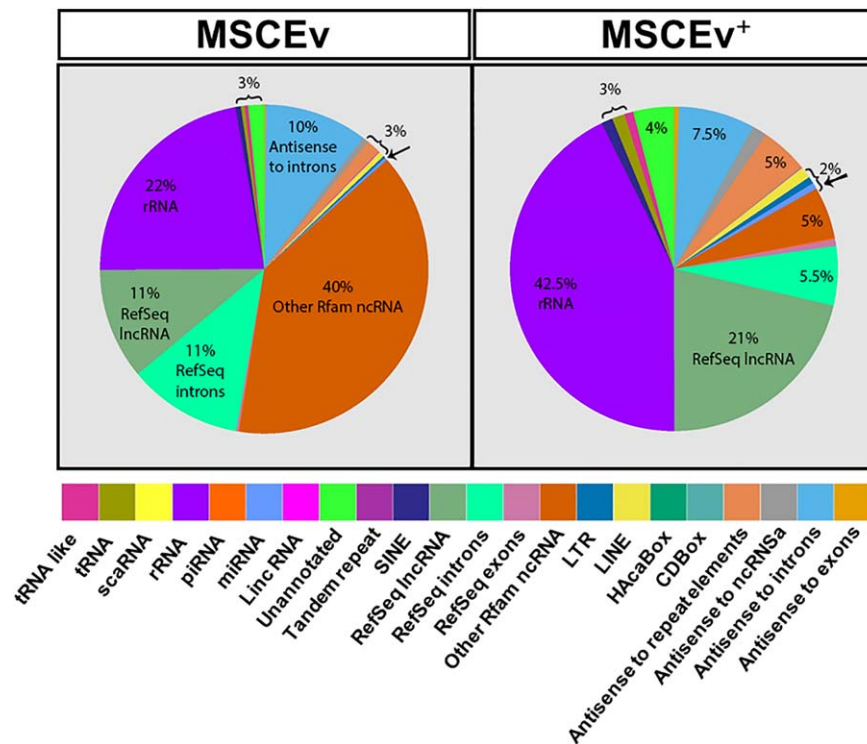


**Figure 4.** Relative MSCEv RNA expression. Next generation sequencing hits were analyzed and grouped into classes of known and predicted nucleic acid types. Presented here are the relative contributions of these classes relative to the total number of sequences for MSCEv (left) and MSCEv<sup>+</sup> (right) normalized to the total number of reads generated. The relative percentage and identification of major categories are shown. The location of miRNA is indicated by the arrow (←). Abbreviations: miRNA, micro RNA; piRNA, piwi-interacting RNA; tRNA, transfer RNA.

resulting in a distinctly different fingerprint (Fig. 4). There is a considerable decrease in the relative abundance of (Rfam ncRNA) sequences in MSCEv<sup>+</sup> compared to MSCEv and an increase in long noncoding RNA sequences (Refseq lncRNA) which have been linked to inflammatory control via several mechanisms [24–27].

miRNA packaged in MSC-derived microvesicles have been shown to have potent immunomodulatory effects [28–30]. A number of mechanisms have been proposed as key mediators of this effect. We identified 11 miRNAs with a greater than 10-fold difference in expression between MSCEv<sup>+</sup> and MSCEv (Supporting Information Table S2). Notably, several of these miRNA have reported functions that are immunomodulatory either directly or indirectly.

#### TNF- $\alpha$ /IFN- $\gamma$ Splenocyte Inhibition Assay

Primary splenocytes were isolated from immunocompetent Sprague-Dawley rats as previously described [19, 23], and activated using either LPS or concanavalin A (ConA) to preferentially stimulate either myeloid cells or T cells, respectively. We found that both MSCEv<sup>+</sup> and MSCEv were capable of significantly reducing the amount of TNF- $\alpha$  and IFN- $\gamma$  accumulated more than 24 hours and 72 hours, respectively. Additionally, MSCEv<sup>+</sup> was capable of significantly decreasing TNF- $\alpha$  and IFN- $\gamma$  compared to MSCEv when  $10^5$  EVs per reaction were added here (Fig. 5). Higher concentrations of EVs tended to demonstrate the same difference without achieving statistical significance. While the degree of TNF- $\alpha$  inhibition and the dose at which significant differences were detected

varied between experiments and preparations of EVs, MSCEv<sup>+</sup> consistently outperformed MSCEv (Fig. 6C).

#### Protein-Based Immunomodulation by Follistatin and Activin

We tentatively explored several mechanisms by which MSCEv<sup>+</sup> may act as homeostatic immunomodulators. We have previously described the nucleic acid profile of the EVs, whereby there are a number of activity-modifying moieties that may be present. Here, we briefly discuss two particular protein-based mechanisms by which EVs may exert immunomodulatory activity.

We have previously demonstrated that MSCs are potent immunomodulators that use COX2 and PGE<sub>2</sub> both in vitro (using the same cytokine inhibition assays as shown in Fig. 5), as well as in vivo, in a traumatic brain injury model [19]. Given this, we additionally assayed the conditioned media from the TNF- $\alpha$  inhibition assay for PGE<sub>2</sub> by ELISA and found that the MSCEv<sup>+</sup> treated coculture contained a remarkable amount of PGE<sub>2</sub> (Fig. 6A) when compared to MSCEv and even reference amniotic fluid derived MSCs, although the source of the PGE<sub>2</sub> cannot be directly determined as directly from MSCEv or from induced splenocytes.

Western blot analysis demonstrated that MSCEv<sup>+</sup> contain dramatically more COX2 compared to MSCEv or empty liposomes, and was also readily detected in serum-derived EVs as a positive control.

In order to determine the contribution of COX2 and PGE<sub>2</sub> to the immunopotency of MSCEv and MSCEv<sup>+</sup>, we repeated

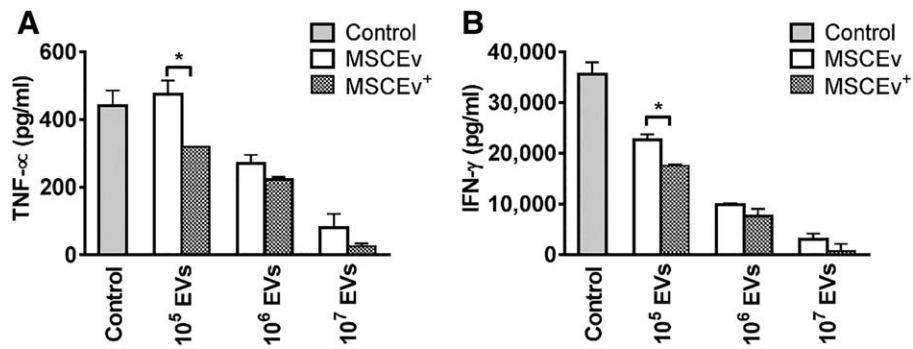


**Figure 5.** TNF- $\alpha$  and IFN- $\gamma$  inhibition assays. Primary rat splenocytes were stimulated with lipopolysaccharide and ConA immediately prior to the addition of EVs or a control and left to incubate overnight. Conditioned media was then assayed by enzyme-linked immunosorbent assay (ELISA) to determine the ability of MSCEv<sup>+</sup> and MSCEv to inhibit accumulation of TNF- $\alpha$  (A). Similarly, EVs were evaluated for their ability to inhibit IFN- $\gamma$  secretion and accumulation from ConA-stimulated splenocytes more than 72 hours (B). \*,  $p < .05$ . Abbreviation: EV, extracellular vesicle.

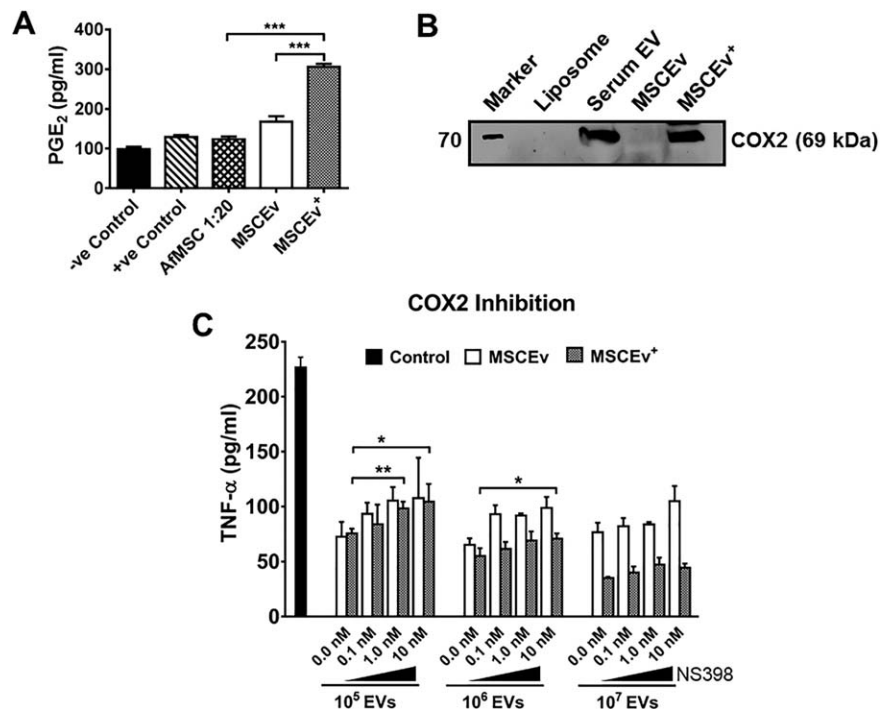


**Figure 6.** PGE<sub>2</sub> and COX2 participate in TNF- $\alpha$  inhibition. Samples of supernatant from the previous TNF- $\alpha$  inhibition assay (Fig. 5A) were assayed for PGE<sub>2</sub> by ELISA (A). EV lysate was then probed for the presence of COX2 by Western blot (B). Primary rat splenocytes were activated with lipopolysaccharide as in (Fig. 5A) and cocultured with increasing amounts of the two EVs in the presence of increasing amounts of a COX2 inhibitor (NS398) for 24 hours. The resulting accumulation of TNF- $\alpha$  was assayed by enzyme-linked immunosorbent assay (ELISA) (C). \*,  $p < .05$ ; \*\*,  $p < .01$ ; \*\*\*,  $p < .001$ . Abbreviations: AfMSC, amniotic fluid derived MSC; EV, extracellular vesicle.

the TNF- $\alpha$  inhibition assay as before (Fig. 5) in the presence of increasing amounts of a COX2 specific inhibitor (NS398) at several dilutions (Fig. 6C). We found that NS398 significantly increased TNF- $\alpha$  using 10<sup>5</sup> EVs from both groups. At higher concentrations, MSCEv demonstrated a much larger response to NS398 in comparison to MSCEv<sup>+</sup>, which became somewhat resistant to the effects of NS398 while still appearing to have a dose-dependent response. Similar effects were observed using a less-specific COX2 inhibitor, indomethacin (data not shown).

As an alternative to COX2/PGE<sub>2</sub> activity, we found significant differences in the expression of Actin A ( $p < .01$ ) and Follistatin ( $p < .001$ ) between MSCEv and MSCEv<sup>+</sup> (Supporting Information Fig. S1), while PAPP-A2 expression was decreased.

These molecules have not been previously reported as components of MSCEv immunobiology.

### Flow Cytometry Characterization of Differential Immune Cell Interaction with EVs

We evaluated the interaction of stimulated immune cells with the EVs using a multiparameter flow cytometry assay to detect the uptake of labeled EVs (Fig. 7). Human PBMCs were isolated from a fresh aspirate and stimulated using LPS or ConA, as in our previous cytokine inhibition assays, or CD3/CD28 beads to more accurately model a physiological inflammatory response (Fig. 7A). Activated PBMC were then cocultured with fluorescently labeled MSCEv or MSCEv<sup>+</sup>,

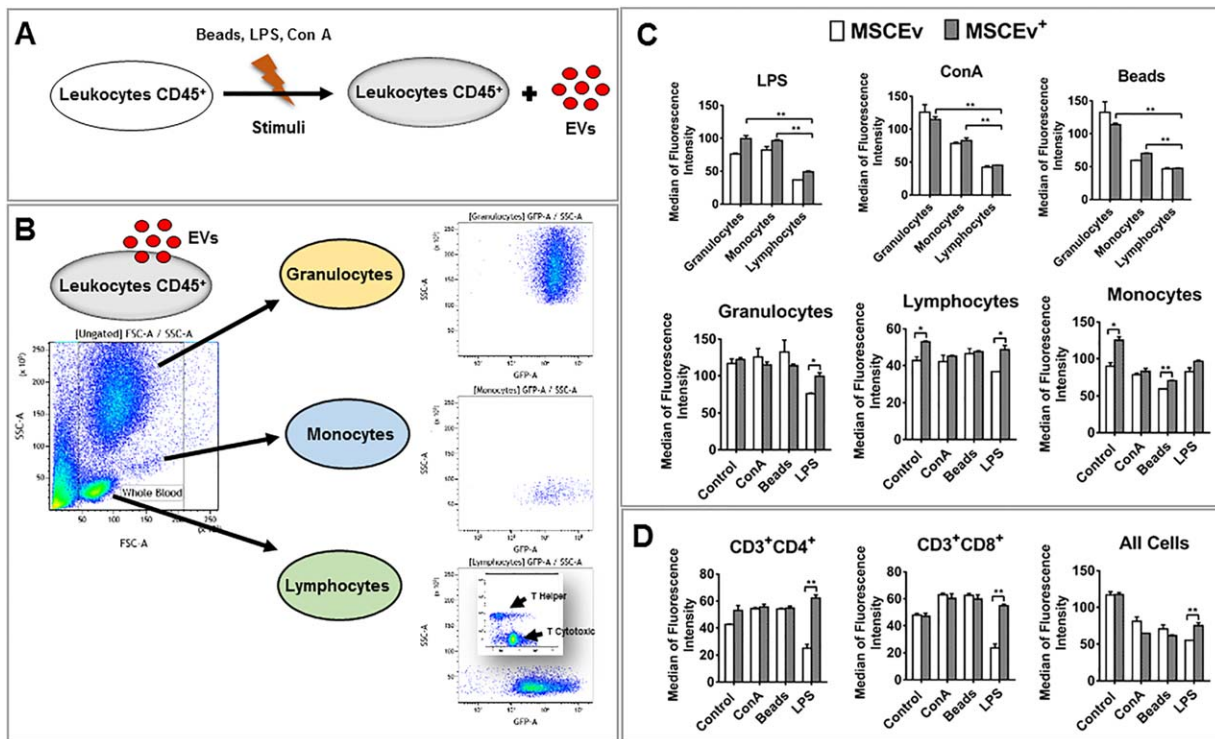


**Figure 7.** MSCEv and MSCEv<sup>+</sup> uptake by human peripheral blood cells. To evaluate the interaction between peripheral blood cells and extracellular vesicles (EVs), we performed a multiparameter, differential uptake assay (A). Cells were activated using LPS, ConA, or beads 24 hours prior to a 2 hours incubation with fluorescently labeled EVs. Cells were then washed to remove unbound or free EVs and analyzed by flow cytometry. Uptake of EV by granulocytes, monocytes, and lymphocytes was determined based on size and characteristic markers (B). In general, all activation methods resulted in reduced uptake when compared to nonstimulated peripheral blood mononuclear cell. Significant reduction in the uptake was observed for the LPS treated cell incubated with activated EVs ( $p = .03$ ). When comparing the three major groups of cells, granulocytes seem to uptake more EVs than monocytes and even fewer EVs were taken up by lymphocytes (C). When analyzing the effect of the EVs within the different cell treatments (LPS, ConA, or beads), only LPS treatment increased the uptake of MSCEv<sup>+</sup> for granulocytes, monocytes, and lymphocytes, including CD4 and CD8 T cells. The ConA or bead treatments did not have that trend (C, D). This could imply a specific interaction mechanism induced by LPS, but not ConA or beads. \*,  $p < .05$ ; \*\*,  $p < .01$ . Abbreviation: LPS, lipopolysaccharide.

immunostained with additional markers, and various myeloid and lymphoid populations were then analyzed for EV uptake.

Stimulating PBMC with beads or ConA (Fig. 7C) resulted in a pattern of higher uptake by the granulocytes, medium uptake by the monocytes, and significantly lower uptake by lymphocytes ( $p < .01$ ), although there was no significant difference between MSCEv<sup>+</sup> and MSCEv. LPS stimulation resulted in significantly higher uptake for the MSCEv<sup>+</sup> compared to MSCEv, with an overall increase in EV uptake by monocytes while there was a decreased uptake by granulocytes. By comparing leukocyte uptake (Fig. 7B), we are able to observe a pattern of high uptake by granulocytes, medium uptake in monocytes, and low uptake in lymphocytes. LPS stimulation seems to decrease uptake only of MSCEv in granulocytes and lymphocytes compared to the other conditions while MSCEv<sup>+</sup> have significantly higher uptake compared to MSCEv. This difference may demonstrate that leukocytes use specificity in differential uptake of EV in inflammatory conditions (Fig. 7C). The same difference in EV uptake was also found in bead-stimulated monocytes. The preference for MSCEv<sup>+</sup> compared to MSCEv is readily apparent when limiting analysis to T cytotoxic (CD3<sup>+</sup> CD8<sup>+</sup>) and T helper (CD3<sup>+</sup> CD4<sup>+</sup>) cells (Fig. 7D). And finally, the difference between EV uptake can even be detected when analyzing whole blood (Fig. 7D), conclusively demonstrating that, while stimulation

of leukocytes tends to decrease EV uptake, there remains a significant difference between MSCEv and MSCEv<sup>+</sup> when PBMC are activated with LPS.

## DISCUSSION

EVs are emerging as critical mediators of an increasing number of biological interactions. They are an important intermediary in cellular communication, carrying numerous molecular, genetic, and subcellular elements that can influence tissue, cell, and molecular function and response [31]. Given this, the therapeutic potential of EVs continues to be a topic of great interest. In this study, we used a unique cGMP-compliant TFF system to isolate and thoroughly characterize EVs released by hMSCs. We additionally demonstrate that MSCs exposed to inflammatory cytokines TNF- $\alpha$  and IFN- $\gamma$  generate EVs with altered protein and nucleic acid composition, along with enhanced immunomodulatory properties.

We demonstrated the anti-inflammatory activity of EVs by an activated rat splenocyte cytokine inhibition assay. This in vitro system has been used in a parallel study to demonstrate a direct correlation between in vitro performance in this assay and in vivo inhibition of neuroinflammation in an experimental model of traumatic brain injury, largely via a COX2/PGE<sub>2</sub>



mediated mechanism [19]. The ability of MSC-derived EVs to replicate some of the efficacy of MSC in this assay strongly implies that EVs are responsible for some of the immunomodulatory activity of MSCs in an inflammatory environment. The increased activity of MSCEv<sup>+</sup> compared to MSCEv is logical in the context that MSC have a dynamic response to their environment, demonstrating multimodal therapeutic activities that include angiogenesis, neuroprotection, and even neurogenesis in addition to immunomodulation [32].

The use of primary immune cells isolated from different animal donors at different times can present some technical difficulties, as evident by the difference in EV activity between Figures 5 and 6C. We consistently must use a dose-response curve in order to capture the differences between MSCEv and MSCEv<sup>+</sup>, as different animals' splenocytes have varied degrees of responsiveness to the super antigen. We have additionally seen "lot" variation in our EVs, in that MSCs from a single master cell bank can produce EVs that have different immunomodulatory "potency," a phenomenon that has been similarly documented with MSCs themselves [19]. We attempted to minimize variation and increase rigor by using absolute counts of EV for our assays, but the differences between EV preparations is evident in the difference in TNF- $\alpha$  inhibition by similar doses of EVs between Figures 5 and 6C. Despite this difference, we have consistently observed that MSCEv and MSCEv<sup>+</sup> are capable of reducing TNF- $\alpha$  and IFN- $\gamma$  across multiple large-scale preparations, and further, that MSCEv<sup>+</sup> have an incremental, but significant, improvement over MSCEv (additional data not shown). It is important to note that MSCEv demonstrate significant immunomodulatory capabilities and MSCEv<sup>+</sup> represent an optimization of that activity.

We observed a striking increase in COX2 expression in the MSCEv<sup>+</sup> compared to MSCEv. This change translated directly to PGE<sub>2</sub> concentration in conditioned media from the activated splenocyte cocultures. The role of COX2 and PGE<sub>2</sub> in EV-based immunomodulation was then confirmed by repeating the activated splenocyte coculture in the presence of a COX2 inhibitor. We readily admit (and demonstrate) that there are a number of other mechanisms by which EVs may exert immunomodulatory activity. For example, we found significant increases in expression of follistatin and activin A and a decrease in PAPP-A2 expression in MSCEv<sup>+</sup> compared to MSCEv as a potential "non-canonical" aspect of EV biology.

Finally, in a multiplexed coculture system, we show that granulocytes have the most robust uptake of MSCEv<sup>+</sup>, though a number of other leukocytes have stimulus-dependent changes in uptake specific to MSCEv<sup>+</sup>. Moreover, we found that LPS-stimulation resulted in a significant increase in MSCEv<sup>+</sup> uptake compared to MSCEv in complete whole blood and more dramatically in several sub-populations. This multiparametric, single tube assay can be adapted to explore future therapeutic applications as well as to tease apart the complex changes that EV are capable of in a mixed leukocyte system.

Given the emerging opportunity for translation into clinical therapies and ultimate therapeutic potential of EVs, their isolation in compliance with existing regulatory frameworks is of major importance. Isolation of EVs using differential ultracentrifugation continues to be the most commonly used and reported method [33–35]. This process is lengthy, inefficient (often <50% of EVs are recovered), and susceptible to

contamination, rendering this approach technically challenging for cGMP manufacturing and clinical translation. Alternatives include EV isolation reagents that precipitate EVs from the media [35], immunoisolation [36, 37], and size exclusion methods like sequential filtration or chromatography [38, 39]. The TFF system we used in this study facilitates efficient isolation of a cGMP-compliant and a well-defined population of EVs [38, 40]. Furthermore, this method has shown minimal effect on the characteristics of the isolated EV population [41]. Notably, the TFF technique is easily adapted to cGMP requirements, streamlining the translation to regulated production of EVs without significant changes. In agreement with previously identified findings [40], our internal quality experiments noted that a secondary ultra-centrifugation step resulted in a large EV loss, resulting in a smaller volume with several orders of magnitude fewer EVs (data not shown).

Irrespective of selection method, EVs should be rigorously characterized to optimize comparisons between studies and increase reproducibility. We used multiple EV characterization parameters including vesicle morphology, quantity and particle size distribution, as well as the expression of specific surface markers and nucleic acid cargo, in addition to immunomodulatory activity, as there have been shown to be notable differences in EVs depending on isolation method [42]. The International Society for Extracellular Vesicles has recommends that the minimum requirement is identification of at least one transmembrane or lipid-bound extracellular protein (such as CD9, CD63, and/or CD81) [43], though there may be variability in individual markers. Given the challenges of working with EVs, and a lack of standardization [44], we feel that thorough characterization and methodology is required. We used commercially available empty liposomes of similar size to EVs as an experimental negative control, along with human serum-derived EVs as a well-defined, positive control, reference. Serum EVs, a mixed population positive control, expressed all commonly-reported EV markers (though the expression of CD63 was low) and liposomal controls were void of markers. We identified CD63 among MSCEv and MSCEv<sup>+</sup> by both Western blotting and flow cytometry. The expression of CD9 and CD81 was varied, possibly secondary to changes associated with MSC stimulation and/or our specific TFF EV isolation processes.

Numerous EV targets and mechanisms of cellular/mechanistic modulation have been proposed with no shortage of new reports. These include (but are not limited to) anti-inflammatory [45] or pro-inflammatory [46] effects, antitumor [47], angiogenesis [48], cytoprotection [49], and tissue/cellular regeneration [50]. It is likely that varied mechanisms are responsible for the different reported activities of EVs. Most relevant to our group's interest, we have found that EVs are capable of immunomodulation similar to MSC. Previous work in a pulmonary inflammation rodent model has shown that human MSC-derived EVs can modulate macrophages, lymphocytes, neutrophils, and eosinophils, along with overall tissue inflammation [51]. Specific immunomodulation through targeted interaction with monocytes, potentially via the delivery of miR-10a, has also been identified [52]. Activin-A and Follistatin have been shown to modulate the inflammatory response (specifically TNF- $\alpha$ ), leading to improved mortality [53].

Additionally, EVs have previously been shown to express COX2 and have varying lipid profiles [54, 55], with some studies even indicating that PGE<sub>2</sub> may be involved in MSCEv activity [56]. Here, we found that EVs use COX2/PGE<sub>2</sub> to decrease TNF- $\alpha$  production in addition to other immunomodulatory mechanisms. Importantly, we demonstrated that we can “stimulate” MSCs to produce EVs containing an increased amount of COX2, that are also capable of drastically increasing the amount of PGE<sub>2</sub> produced during coculture with inflamed cells. This simple optimization step would often be invisible, as the moment MSCs are introduced into an inflamed environment (in culture, in a microenvironment, or even in vivo from systemic cytokines) they could rapidly change their MSCEv to MSCEv<sup>+</sup> with properties similar to the ones we report here. This can effectively render many pre-treatment steps moot and obscure putative mechanisms of efficacy for both cells and EVs.

The specific mechanism by which EVs target specific cells and deliver cargo is not well understood. In this study, we report selective and context-specific uptake of different EVs by activated leukocytes, similar to a differentially expressed receptor-ligand system. Using a multiplexed assay, we were able to rapidly determine the relative uptake of labeled EVs between lymphoid and myeloid populations. Furthermore, we observed a change in EV uptake as a response to different stimuli, including super antigens (LPS and ConA) and CD3/CD28 beads to provide a more physiologically relevant activation of T cells. While the differences in uptake between granulocytes, monocytes, and lymphocytes can be somewhat explained by their relative phagocytic activity, the differences in uptake between stimulated and nonstimulated leukocyte populations warrants further investigation. Similarly, the specific mechanism of EV uptake that created significant differences between MSCEv and MSCEv<sup>+</sup> in control and LPS-stimulated leukocyte subpopulations, especially T cell populations, provides an interesting clue toward potential mechanisms of efficacy and targeting.

There are several important limitations to this investigation. The data presented in this study was generated using MSCs isolated, expanded, and cryopreserved in a master cell bank from a single female donor at passage 3. Three individual preparations of MSCEv and MSCEv<sup>+</sup> were then prepared, characterized, and tested for activity. While EV demonstrated consistent immunomodulatory activity, the potency per EV varied. While these differences could be caused by errors by the nanoparticle analyzer, differences in reactivity of splenocytes between animals, and any number of other factors, our own experiences with the heterogeneity of MSC and enigmatic changes in their “potency” forces us to consider that there remain unknown elements that likely affect EVs as well. We tested EVs derived from four additional donors generated using the same treatments described here and have found a consistent increase in immunomodulatory activity as a result of TNF- $\alpha$  and IFN- $\gamma$  stimulation in all but one MSC donor (data not shown). Despite our attempts to standardize our culture, isolation, and characterization techniques, EVs isolated from primary cells, and particularly MSC, will remain heterogeneous with unexplainable differences in potency. Alternative sources of EVs, such as those derived from a single, non-stem cell line, may be useful to generate a consistent EV product that is capable of targeting a specific cell for a more reproducible study. Ultimately, additional, well-controlled experimental

animal studies (and subsequent human trials) will be required to conclusively demonstrate the efficacy of MSCEv<sup>+</sup> in vivo.

Our overall hypothesis, that MSCs would respond to inflammatory stimuli by producing EVs with greater anti-inflammatory activity, is consistent with our observations. This strategy can be adapted to a number of other current and future applications of MSCs and MSC-derived EV. For example, by preconditioning MSC in hypoxia prior to harvesting EV, EV may be optimized for ischemic injuries.

## CONCLUSION

We have shown that EV isolation using TFF is a cGMP-compliant process that is relatively simple, reliable, and scalable. We identified that pre-treatment of MSCs with TNF- $\alpha$  and IFN- $\gamma$  results in EVs with a distinctly different profile compared to naïve MSCEv. While both EV preparations attenuate inflammatory cytokines from splenocytes, MSCEv<sup>+</sup> had an enhanced ability to mitigate TNF- $\alpha$  and IFN- $\gamma$  release following activation. Among several potential mechanisms of action, we show that MSCEv<sup>+</sup> use PGE<sub>2</sub> via COX2 mechanisms to reduce inflammatory cytokines in vitro. Finally, we show evidence of stimulus-dependent and cell-specific internalization of EVs by PBMCs and whole blood, where MSCEv and MSCEv<sup>+</sup> were preferentially taken up by different leukocyte populations after exposure to different antigens.

## ACKNOWLEDGMENTS

This study was supported by grants Center for Clinical and Translational Sciences Training Award, University of Texas McGovern Medical School (5KL2-TR000370-10) (M.T.H.); Ladybug (C.S.C. and M.T.H.); Glassell Family Stem Cell Research Fund. We acknowledge Ansh Labs support with Activin-A, follistatin, and PAPP-A2 assays.

## AUTHOR CONTRIBUTIONS

M.T.H.: conception and design, financial support, administrative support, data analysis and interpretation, manuscript writing, final approval of manuscript; C.S.C.: conception and design, data analysis and interpretation, manuscript writing, final approval of manuscript; S.D.O.: conception and design, financial support, administrative support, collection and/or assembly of data, data analysis and interpretation, manuscript writing, final approval of manuscript; A.K.S.: administrative support, provision of study material or patients, collection and/or assembly of data, data analysis and interpretation, manuscript writing, final approval of manuscript; S.Z., H.B., K.S.P., and N.E.T.F.: provision of study material or patients, collection and/or assembly of data, data analysis and interpretation, final approval of manuscript; J.V.V.: collection and/or assembly of data, data analysis and interpretation, final approval of manuscript; K.A.R.: collection and/or assembly of data, data analysis and interpretation, manuscript writing, final approval of manuscript.

## DISCLOSURE OF POTENTIAL CONFLICTS OF INTEREST

The authors indicated no potential conflicts of interest.

## REFERENCES

- 1 Harting MT, Jimenez F, Xue H. Intravenous mesenchymal stem cell therapy for traumatic brain injury. *J Neurosurg* 2009;110:1189–1197.
- 2 Kota DJ, Prabhakara KS, van Brummen AJ et al. Propranolol and mesenchymal stromal cells combine to treat traumatic brain injury. *STEM CELLS TRANSLATIONAL MEDICINE* 2016;5:33–44.
- 3 Lee RH, Seo MJ, Reger RL et al. Multipotent stromal cells from human marrow home to and promote repair of pancreatic islets and renal glomeruli in diabetic NOD/scid mice. *Proc Natl Acad Sci USA* 2006;103:17438–17443.
- 4 Srivastava AK, Bulte CA, Shats I et al. Co-transplantation of syngeneic mesenchymal stem cells improves survival of allogeneic glial-restricted precursors in mouse brain. *Exp Neurol* 2016;275:154–161.
- 5 Boomsma RA, Geenen DL, Hofmann TG. Mesenchymal stem cells secrete multiple cytokines that promote angiogenesis and have contrasting effects on chemotaxis and apoptosis. *PLoS One* 2012;7:e35685.
- 6 van der Pol E, Böing AN, Harrison P et al. Classification, functions, and clinical relevance of extracellular vesicles. *Pharmacol Rev* 2012;64:676–705.
- 7 Budnik V, Ruiz-Cañada C, Wendler F. Extracellular vesicles round off communication in the nervous system. *Nat Rev Neurosci* 2016;17:160–172.
- 8 Koniusz S, Andrzejewska A, Muraca M et al. Extracellular vesicles in physiology, pathology, and therapy of the immune and central nervous system, with focus on extracellular vesicles derived from mesenchymal stem cells as therapeutic tools. *Front Cell Neurosci* 2016;10:109.
- 9 Camussi G, Deregis MC, Bruno S et al. Exosomes/microvesicles as a mechanism of cell-to-cell communication. *Kidney Int* 2010;78:838–848.
- 10 Lai RC, Tan SS, Teh BJ et al. Proteolytic potential of the MSC exosome proteome: Implications for an exosome-mediated delivery of therapeutic proteasome. *Int J Proteomics* 2012;2012:971907.
- 11 Vlassov AV, Magdaleno S, Setterquist R et al. Exosomes: Current knowledge of their composition, biological functions, and diagnostic and therapeutic potentials. *Biochim Biophys Acta* 2012;1820:940–948.
- 12 Camussi G, Deregis MC, Cantaluppi V. Role of stem-cell-derived microvesicles in the paracrine action of stem cells. *Biochem Soc Trans* 2013;41:283–287.
- 13 Tetta C, Ghigo E, Silengo L et al. Extracellular vesicles as an emerging mechanism of cell-to-cell communication. *Endocrine* 2013;44:11–19.
- 14 Baglio SR, Pegtel DM, Baldini N. Mesenchymal stem cell secreted vesicles provide novel opportunities in (stem) cell-free therapy. *Front Physiol* 2012;3:359.
- 15 Li T, Yan Y, Wang B et al. Exosomes derived from human umbilical cord mesenchymal stem cells alleviate liver fibrosis. *Stem Cells Dev* 2013;22:845–854.
- 16 Butler J, Epstein SE, Greene SJ et al. Intravenous allogeneic mesenchymal stem cells for non-ischemic cardiomyopathy: Safety and efficacy results of a phase II-A randomized trial. *Circ Res* 2017;120:332–340.
- 17 Fischer UM, Harting MT, Jimenez F et al. Pulmonary passage is a major obstacle for intravenous stem cell delivery: The pulmonary first-pass effect. *Stem Cells Dev* 2009;18:683–692.
- 18 Sekiya I, Larson BL, Smith JR et al. Expansion of human adult stem cells from bone marrow stroma: Conditions that maximize the yields of early progenitors and evaluate their quality. *STEM CELLS* 2002;20:530–541.
- 19 Kota DJ, Prabhakara KS, Toledano-Furman N et al. Prostaglandin E2 indicates therapeutic efficacy of mesenchymal stem cells in experimental traumatic brain injury. *STEM CELLS* 2017;35:1416–1430.
- 20 Yang M, Chen J, Su F et al. Microvesicles secreted by macrophages shuttle invasion-potentiating microRNAs into breast cancer cells. *Mol Cancer* 2011;10:117.
- 21 Palanisamy V, Sharma S, Deshpande A et al. Nanostructural and transcriptomic analyses of human saliva derived exosomes. *PLoS One* 2010;5:e8577.
- 22 Olsen AB, Hetz RA, Xue H et al. Effects of traumatic brain injury on intestinal contractility. *Neurogastroenterol Motil* 2013;25:593–e463.
- 23 Kota DJ, DiCarlo B, Hetz RA et al. Differential MSC activation leads to distinct mononuclear leukocyte binding mechanisms. *Sci Rep* 2015;4:4565.
- 24 Mao X, Su Z, Mookhtiar AK. LncRNA: A versatile regulator of the NF-kappaB signaling circuit. *Immunology* 2016;150:379–388.
- 25 Elling R, Chan J, Fitzgerald KA. Emerging role of long noncoding RNAs as regulators of innate immune cell development and inflammatory gene expression. *Eur J Immunol* 2016;46:504–512.
- 26 Heward JA, Lindsay MA. Long non-coding RNAs in the regulation of the immune response. *Trends Immunol* 2014;35:408–419.
- 27 Robbins PD, Dorronsoro A, Booker CN. Regulation of chronic inflammatory and immune processes by extracellular vesicles. *J Clin Invest* 2016;126:1173–1180.
- 28 Ti D, Hao H, Fu X et al. Mesenchymal stem cells-derived exosomal microRNAs contribute to wound inflammation. *Sci China Life Sci* 2016;59:1305–1312.
- 29 Ti D, Hao H, Tong C et al. LPS-preconditioned mesenchymal stromal cells modify macrophage polarization for resolution of chronic inflammation via exosome-shuttled let-7b. *J Transl Med* 2015;13:308.
- 30 Katsuda T, Kosaka N, Takeshita F et al. The therapeutic potential of mesenchymal stem cell-derived extracellular vesicles. *Proteomics* 2013;13:1637–1653.
- 31 Raposo G, Stoorvogel W. Extracellular vesicles: Exosomes, microvesicles, and friends. *J Cell Biol* 2013;200:373–383.
- 32 Ropper AE, Thakor DK, Han I et al. Defining recovery neurobiology of injured spinal cord by synthetic matrix-assisted hMSC implantation. *Proc Natl Acad Sci USA* 2017;114:E820–E829.
- 33 Raposo G, Nijman HW, Stoorvogel W et al. B lymphocytes secrete antigen-presenting vesicles. *J Exp Med* 1996;183:1161–1172.
- 34 Thery C, Amigorena S, Raposo G et al. Isolation and characterization of exosomes from cell culture supernatants and biological fluids. *Curr Protoc Cell Biol* 2006;30:3.22.1–3.22.29.
- 35 Schageman J, Zeringer E, Li M et al. The complete exosome workflow solution: From isolation to characterization of RNA cargo. *BioMed Res Int* 2013;2013:253957.
- 36 Clayton A, Court J, Navabi H et al. Analysis of antigen presenting cell derived exosomes, based on immuno-magnetic isolation and flow cytometry. *J Immunol Methods* 2001;247:163–174.
- 37 Nakai W, Yoshida T, Diez D et al. A novel affinity-based method for the isolation of highly purified extracellular vesicles. *Sci Rep* 2016;6:33935.
- 38 Lamparski HG, Metha-Damani A, Yao JY et al. Production and characterization of clinical grade exosomes derived from dendritic cells. *J Immunol Methods* 2002;270:211–226.
- 39 Kim DK, Nishida H, An SY et al. Chromatographically isolated CD63+CD81+ extracellular vesicles from mesenchymal stromal cells rescue cognitive impairments after TBI. *Proc Natl Acad Sci USA* 2016;113:170–175.
- 40 Heinemann ML, Ilmer M, Silva LP et al. Benchtop isolation and characterization of functional exosomes by sequential filtration. *J Chromatogr A* 2014;1371:125–135.
- 41 Gamez-Valero A, Monguio-Tortajada M, Carreras-Planella L et al. Size-exclusion chromatography-based isolation minimally alters extracellular vesicles' characteristics compared to precipitating agents. *Sci Rep* 2016;6:33641.
- 42 Taylor DD, Shah S. Methods of isolating extracellular vesicles impact downstream analyses of their cargoes. *Methods* 2015;87:3–10.
- 43 Lotvall J, Hill AF, Hochberg F et al. Minimal experimental requirements for definition of extracellular vesicles and their functions: A position statement from the International Society for extracellular vesicles. *J Extracell Vesicles* 2014;3:26913.
- 44 Gardiner C, Di Vizio D, Sahoo S et al. Techniques used for the isolation and characterization of extracellular vesicles: Results of a worldwide survey. *J Extracell Vesicles* 2016;5:32945.
- 45 Yang J, Liu XX, Fan H et al. Extracellular vesicles derived from bone marrow mesenchymal stem cells protect against experimental colitis via attenuating colon inflammation, oxidative stress and apoptosis. *PLoS One* 2015;10:e0140551.
- 46 Lee H, Zhang D, Zhu Z et al. Epithelial cell-derived microvesicles activate macrophages

and promote inflammation via microvesicle-containing microRNAs. *Sci Rep* 2016;6:35250.

**47** Katakowski M, Chopp M. Exosomes as tools to suppress primary brain tumor. *Cell Mol Neurobiol* 2016;36:343–352.

**48** Kim CW, Lee HM, Lee TH et al. Extracellular membrane vesicles from tumor cells promote angiogenesis via sphingomyelin. *Cancer Res* 2002;62:6312–6317.

**49** Zhou Y, Fang L, Yu Y et al. Erythropoietin protects the tubular basement membrane by promoting the bone marrow to release extracellular vesicles containing tPA-targeting miR-144. *Am J Physiol Renal Physiol* 2016;310:F27–F40.

**50** Silva AM, Teixeira JH, Almeida MI et al. Extracellular vesicles: Immunomodulatory

messengers in the context of tissue repair/regeneration. *Eur J Pharm Sci* 2016;98:86–95.

**51** Cruz FF, Borg ZD, Goodwin M et al. Systemic administration of human bone marrow-derived mesenchymal stromal cell extracellular vesicles ameliorates aspergillus hyphal extract-induced allergic airway inflammation in immunocompetent mice. *STEM CELLS TRANSLATIONAL MEDICINE* 2015;4:1302–1316.

**52** Njock MS, Cheng HS, Dang LT et al. Endothelial cells suppress monocyte activation through secretion of extracellular vesicles containing antiinflammatory microRNAs. *Blood* 2015;125:3202–3212.

**53** Jones KL, Mansell A, Patella S et al. Activin A is a critical component of the inflammatory response, and its binding protein, follistatin, reduces mortality in endotoxemia.

*Proc Natl Acad Sci USA* 2007;104:16239–16244.

**54** Deng ZB, Zhuang X, Ju S et al. Exosome-like nanoparticles from intestinal mucosal cells carry prostaglandin E2 and suppress activation of liver NKT cells. *J Immunol* 2013;190:3579–3589.

**55** Subra C, Grand D, Laulagnier K et al. Exosomes account for vesicle-mediated transcellular transport of activatable phospholipases and prostaglandins. *J Lipid Res* 2010;51:2105–2120.

**56** Liu J, Kuwabara A, Kamio Y et al. Human mesenchymal stem cell-derived microvesicles prevent the rupture of intracranial aneurysm in part by suppression of mast cell activation via a pge2-dependent mechanism. *STEM CELLS* 2016;34:2943–2955



See [www.StemCells.com](http://www.StemCells.com) for supporting information available online.